

Takuro Koike

Department of Electronics
Tamagawa University
Machida, Tokyo 194, JapanABSTRACT

The theory of the magnetostatic volume and surface wave propagation within obliquely magnetized YIG films and a correction to the previously reported results are discussed. The experimental confirmation of the new theory is also given.

Introduction

In recent years, the magnetostatic wave propagation in thin YIG films has gained considerable attention and some device applications as well as theoretical treatments have been reported.¹⁻⁸

In this report, we describe a general treatment of the volume wave (VW) and the surface wave (SW) propagations in thin YIG films at an oblique magnetic field. Although the dispersion equations for the VW and the SW within obliquely magnetized YIG films have been discussed by some authors,^{2,4,5} no detailed treatment of the group delay time per unit length T_d has been given. As pointed out by the author,^{7,8} the dispersion of T_d directly reflects the passband characteristics of magnetostatic wave devices and is essentially important for the design of the devices.

We also describe some experimental results which confirm the new theoretical treatment in this report.

Theory

The schematic coordinate systems and the layered structure to be analyzed are shown in Fig. 1 (a), (b), and the inset, respectively. In the case (a), the external magnetic field H_0 is at an arbitrary angle θ to the z -axis and is in the parallel plane (x - y) to the y -axis. In the case (b), H_0 is at an arbitrary angle φ to the z -axis and is in the perpendicular plane (x - z) to the y -axis. In this case, the internal magnetic field H_i is not collinear with H_0 due to demagnetizing effect. If we write the angle between H_i and the z -axis as θ , the following relations are satisfied.^{2,5}

$$\begin{aligned} H_0 \cos \varphi &= H_i \cos \theta \\ 2H_0 \sin (\varphi - \theta) &= 4\pi M_s \sin 2\theta. \end{aligned} \quad (1)$$

Here $4\pi M_s$ is the saturation magnetization of the sample. The values of H_i and θ for given H_0 and φ are obtained by using an iterative procedure.

Using the generalized permeability tensors obtained by the coordinate transformations and assuming the magnetostatic potentials of the forms:

$$\begin{aligned} \phi_I &= A \cosh \{ |k| (x - \frac{d}{2} - t_1) \} e^{-iky}, \\ \phi_{II} &= \{ B e^{\alpha |k| x} + C e^{-\alpha |k| x} \} e^{-iky}, \\ \phi_{III} &= D \cosh \{ |k| (x + \frac{d}{2} + t_2) \} e^{-iky}, \end{aligned} \quad (2)$$

where k is the wave number in the y direction, we obtain the following unified dispersion equation

$$e^{-2\alpha |k| d} = \frac{(a\mu_1 + s\mu_2 \cos \theta + \tanh |k| t_1)(a\mu_1 - s\mu_2 \cos \theta + \tanh |k| t_2)}{(a\mu_1 - s\mu_2 \cos \theta - \tanh |k| t_1)(a\mu_1 + s\mu_2 \cos \theta - \tanh |k| t_2)}, \quad (3)$$

where $s = k/|k|$ takes on the value ± 1 depending on the $\pm y$ direction of the wave propagation. The value of a

is determined by the following relations:

$$\begin{aligned} a^2 &= \alpha^2 = \cos^2 \theta + \sin^2 \theta / \mu_1 \text{ for the case (a);} \\ a^2 &= \alpha^2 = \cos^2 \theta + \sin^2 \theta / \mu_1 \text{ for the case (b).} \end{aligned} \quad (4)$$

The other relevant parameters are given by

$$\begin{aligned} \mu_1 &= 1 - \Omega_H / (\Omega^2 - \Omega_H^2), \quad \mu_2 = \Omega / (\Omega^2 - \Omega_H^2); \\ \Omega_H &= \omega_C / \omega_M, \quad \Omega = \omega / \omega_M, \\ \omega_C &= \gamma H_i, \quad \omega_M = \gamma (4\pi M_s), \end{aligned} \quad (5)$$

where $\gamma/2\pi$ is the gyromagnetic ratio (2.8 GHz/kOe).

The behaviors of propagating waves can be analyzed by solving Eq. (3) with the aid of Eqs. (4) and (5). The VW propagation is obtained for $a^2 < 0$ and the SW propagation is obtained for $a^2 > 0$. The group delay time per unit length T_d can be calculated numerically by the relation:

$$T_d = \lim_{\Delta k \rightarrow 0} (\Delta \omega / \Delta k)^{-1}. \quad (6)$$

In Fig. 2 and Fig. 3, the dispersion curves and the group delay curves for the two cases are shown for $H_0 = 3000$ Oe, $d = 10 \mu\text{m}$, and $t_1, t_2 \rightarrow \infty$. The condition of infinite dielectric layer thickness is sufficient as long as we discuss the position of passbands on the frequency axis.⁷ From the theoretical results we find that a part of the dispersion curves for the case (a) are similar to those of the VW reported earlier⁴ but that the curves for the case (b) are different from those reported by Miller⁵ even if the difference of the thickness of the dielectric layer is taken into account. His calculated results are incorrect. In the case (b), H_i decreases as φ is increased from 0° to 90° due to demagnetizing effect. This should move the upper band edge of the SW and the lower band edge of the VW toward lower frequencies. Therefore, the total passband including the transition frequency from the VW to the SW should move toward lower frequencies as φ is increased from 0° to 90° . While in the case (a), the upper band edge of the SW and the lower band edge of the VW also move toward lower frequencies as θ is increased from 0° to 90° , but the transition frequency remains constant.

Experimental Results

The experiments were performed on a sample of (LaY)IG ($4\pi M_s = 1760$ Oe, $\Delta a^2 = 0$, $d = 15.05 \mu\text{m}$) which was mounted in a 50Ω microstrip line circuit made on a copper-clad teflon fiberglass plate of thickness 0.6 mm. The transduction was achieved through the use of $25 \mu\text{m}$ Al wires flipped over the surface of the sample. The path length was kept at 8 mm for all the experiments.

In Fig. 4, the experimental results for various values of θ and φ at $H_0 = 1845$ Oe, measured by using a microwave sweep oscillator (HP 693A) and a power meter (HP 436A/8484A +30 dB attenuator) combined with a D-A converter (HP 59303A), are shown. Since the theoretical dispersion curves for these cases are similar to those shown in Figs. 2 and 3, only the theoretical passbands corresponding to the experimental results

($T_d \leq 0.465 \mu\text{s/cm}$) are indicated by the shaded areas on the horizontal frequency axes.

In the case (a), the signals in the intermediate angles of θ are not detected well, but the detected signals for small values of θ clearly show the reduction of bandwidth of the SW as predicted by the theory when θ is increased from 0° . The signal detected at $\theta=90^\circ$ is obviously below the transition frequency and corresponds to the VW propagation.

On the contrary to these results, the detected signals for the case (b) shift toward lower frequencies as φ is increased from 0° . The results agree well with the behaviors of the group delay curves for various angles of φ as predicted by the theory in this report.

Conclusion

We have developed a unified theoretical analysis of the magnetostatic wave propagation within obliquely magnetized YIG films. We have also discussed a correction to the previously reported results by Miller.⁵ The new theory was confirmed experimentally for various angles of the external magnetic field. These results will be very useful for future device applications.

Acknowledgment

The author would like to thank Dr. Y. Kino of the Matsushita Electronic Components Co., Ltd. for supplying the material used in the experiments. The author would also like to thank Prof. M. Asanuma of Tamagawa University for valuable discussions.

This work was partially supported by the Hōsō-Bunka Foundation (Japan Broadcasting Corporation).

References

1. R. D. Damon and J. R. Eshbach, "Magnetostatic Modes of a Ferromagnet Slab," *J. Phys. Chem. Solids*, 19, 308-320, 1961.
2. W. Schilz, "Spin-Wave Propagation in Epitaxial YIG Films," *Philips Res. Repts.*, 28, 50-65, 1973.
3. J. M. Owens, R. L. Carter and C. V. Smith, Jr and J. H. Collins, "Magnetostatic Waves, Microwave SAW?," *IEEE 1980 Ultrasonics Symposium Proc.*, 506-513, 1980.
4. N. D. J. Miller, "Non-Reciprocal Propagation of Magnetostatic Volume Waves," *Phys. Stat. Sol.*, 59 593-600, 1977.
5. N. D. J. Miller, "Non-Reciprocal Magnetostatic Volume Waves," *IEEE Trans. Magnetics*, MAG-14, 829-831, 1978.
6. T. Koike, "Tunable Bandpass Filters Utilizing the Magnetostatic Wave Propagation," *IEEE 1978 Ultrasonics Symposium Proc.*, 689-692, 1978.
7. T. Koike, "Tunable Low-Loss Microwave Filters up to X-Band Utilizing the Magnetostatic Surface Wave Propagation," *IEEE 1979 Ultrasonics Symposium Proc.*, 810-815, 1979.
8. T. Koike, "Effects of Directional Coupling on the Magnetostatic Surface Wave Propagation," *IEEE 1980 Ultrasonics Symposium Proc.*, 552-556, 1980.

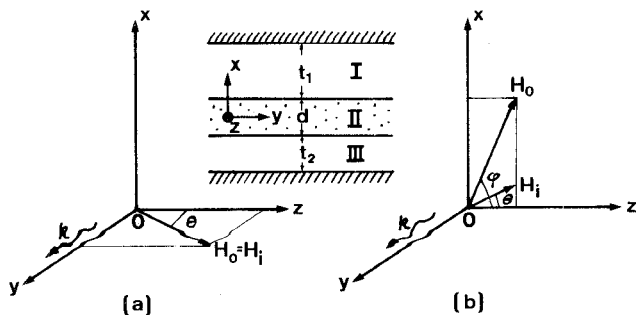


Fig. 1 Schematic coordinate systems.
Inset: Layered structure model.

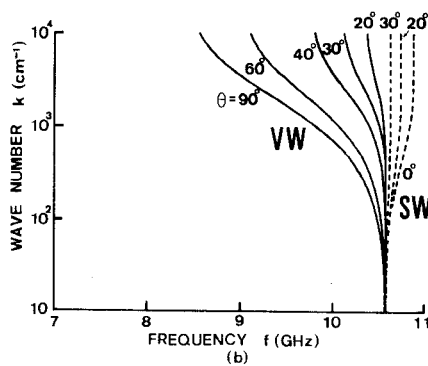
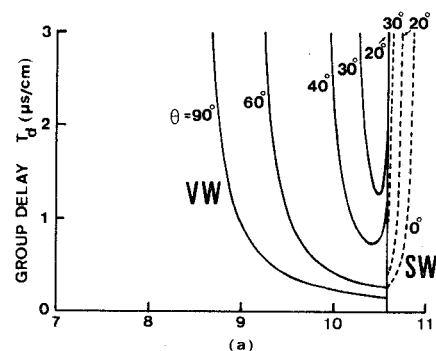


Fig. 2 Dispersion curves for the case (a).
 $H_0=3000 \text{ Oe}$. $d=10 \mu\text{m}$. $t_1, t_2 \rightarrow \infty$.

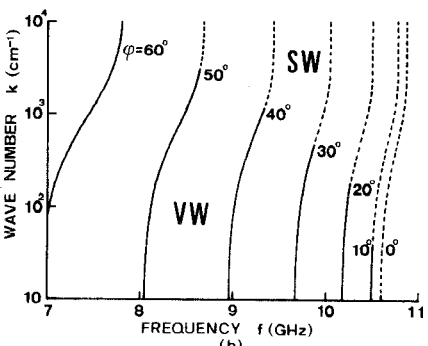
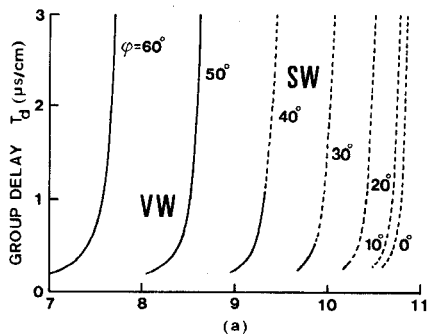


Fig. 3 Dispersion curves for the case (b).
 $H_0=3000 \text{ Oe}$. $d=10 \mu\text{m}$. $t_1, t_2 \rightarrow \infty$.

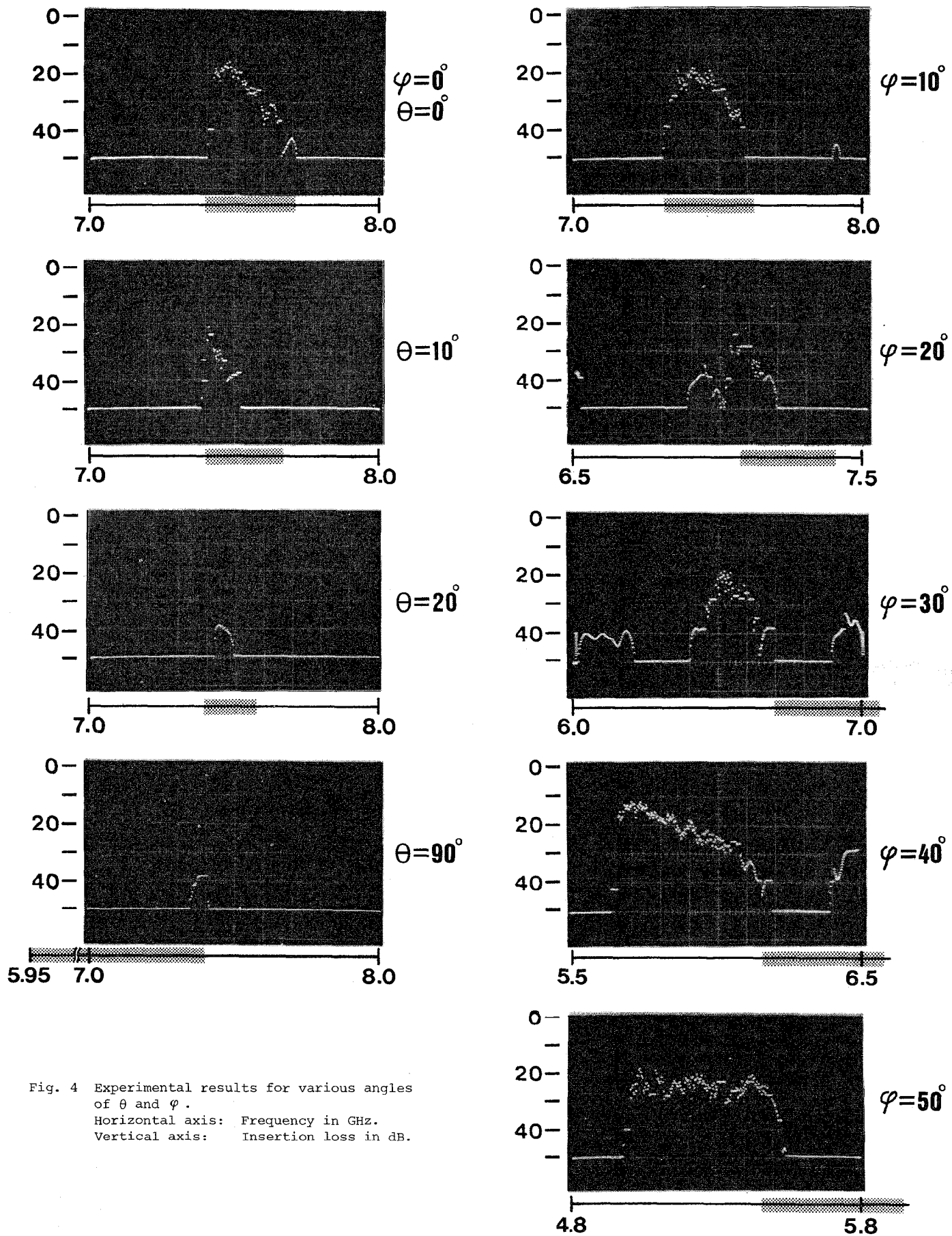


Fig. 4 Experimental results for various angles of θ and φ .
 Horizontal axis: Frequency in GHz.
 Vertical axis: Insertion loss in dB.